Nomenclature

a_i = cost coefficient for ith true batch unit
$\overline{a_i}$ = $a_i W^{\alpha_i}$
A = constant defined by Equation 15
A_H = heat transfer area of exchanger
b_k = cost coefficient for kth semicontinuous unit
$\overline{b_k}$ = $b_k W^{\beta_k}$
C_H = cost of exchanger of A_H ft^2
C_{HS} = cost of exchanger of A_{HS} ft^2
C_i = cost of ith unit
C_P = cost of pump and drive of X hp
C_{PS} = cost of pump and drive of X_S hp
C_R = cost of reactor of V_R ft^3
C_{RS} = cost of reactor of V_S ft^3
F_H, F_P, F_R = proportionality constants relating product volume and volume handled by heat exchanger, pump, reactor, respectively
I = total equipment cost for batch plant
M = number of true batch units
N = number of semicontinuous units
R = number of semicontinuous subtrains
t_i = residence time for ith true batch unit
T = over-all batch cycle time
V = product volume per batch
W = plant production capacity
α_i = cost exponent for ith true batch unit
β_k = cost exponent for kth semicontinuous unit
$\overline{\theta_k}$ = time associated with kth semicontinuous unit
θ_L = time required for Lth semicontinuous subtrain
τ_j = cycle time for jth subbatch train

Literature Cited

Bauman, H. C., "Fundamentals of Cost Engineering in the Chemical Industry," pp. 42–76, Reinhold, New York, 1964.
Duffin, J. R., Peterson, E. L., Zener, C. M., "Geometric Programming," pp. 11, 83, Wiley, New York, 1967.
Ketner, S., American Cyanamid Co., unpublished work, 1960.
Muller, D. E., *Math. Table Aids Comp.* **10**, 208 (1956).

RECEIVED for review November 24, 1969
ACCEPTED May 8, 1970

Flow Pulsation Generator for Pilot-Scale Studies

Charles R. Milburn[1] **and Malcolm H. I. Baird**

Chemical Engineering Department, McMaster University, Hamilton, Ontario, Canada

An air-pulsing technique involving no mechanical moving parts was applied to water flows in ¾- and 2-inch pipes at time-average Reynolds numbers from 3000 to 66,000. The frequency (0.35 to 1.1 cycles per second) and displacement (up to 2.5 feet) are sufficient to cause flow reversal. A numerical technique for predicting the pulsator performance has been developed, but its accuracy is limited by uncertainties about two-phase flow. In its present form, the technique gives a conservative estimate of pulsation intensity.

FLUID PULSATION as an aid to processing has been of interest to researchers ever since the first patent on pulsed extraction was taken out by Van Dijck (1935). Pulsed heat transfer has been studied widely since the first paper by Martinelli (Martinelli *et al.*, 1943), and has been reviewed by Lemlich (1961). In the last ten years, the effects of pulsation on other processes such as absorption (Ziolkowski and Filip, 1963), distillation (McGurl and Maddox, 1967), and fluidization (Massimilla *et al.*, 1966) have been investigated. Such work has been reviewed by Baird (1966). In the majority of cases, pulsation increased the rate of the process compared with unpulsed operation.

However, fluid pulsation has rarely been applied industrially in chemical engineering, with the exception of pulsed solvent extraction. The reason for this anomaly is that extraction is unique in requiring small amplitudes, less than 0.5 inch as a rule, for a good improvement in efficiency. Other processes such as heat transfer require higher intensity pulsations before any appreciable improvement is seen. The generation of intense pulsations on a large scale introduces problems of cavitation and mechanical moving parts, and the question of power consumption becomes important.

Air pulsing, first proposed by Thornton (1954) for pulsed solvent extraction, provides an answer to the first two problems. The air acts as a barrier between the process liquid and any moving parts (piston or bellows) and prevents rapid changes in pressure. Baird (1967) developed an air-pulsing technique which requires no moving parts and depends instead on the unstable alternating discharge of air and liquid from an orifice. This technique has been used by Baird *et al.* (1968) to pulse a solvent extraction column at low amplitudes. As the operating frequency is close to the natural frequency of the system, the power consumption for given intensity is near minimum.

[1] Present address, Ashland Oil Co., Ashland, Ky. 41101

This paper describes an extension of the above technique to provide high intensity pulsation of a turbulent flow of water such as might exist in a commercial heat exchanger. A numerical routine for prediction of amplitude and frequency has also been developed by Milburn (1969). It is felt that such an approach is of more fundamental value than the empirical correlations originally proposed by Baird (1967).

Experimental Procedure

The apparatus shown in Figure 1 is essentially a water circulation loop comprising a reservoir, a pump, the pulsation system, and the "process equipment." The latter is represented in this work by a length of pipe and a gate valve by means of which the frictional effects can be varied. The circulating pump is a variable-speed positive-displacement rotary type (Moyno, Model 2L6).

In normal operation, the steady flow delivered by the pump is fed to the process equipment, but the flow line is also connected to an air-filled surge volume shown on the left of Figure 1, which can absorb flow oscillations. There is no net liquid or air flow to or from the upstream surge; its purpose is solely to permit flow pulsations in the process equipment, even though the feed from the pump is steady.

The liquid flow leaving the process equipment is connected to a downstream surge tank of similar design to the upstream tank. The downstream surge volume is, however, fed with a steady supply of air, metered by a rotameter as shown. This air and the liquid flow are discharged to atmosphere through a relatively small orifice in the vertical rise tube. The discharge is deflected by a return tube as shown and re-enters the reservoir.

The mode of pulsation has been explained by Baird (1967) for a simpler case. Consider an initial condition where the liquid level in the downstream riser is above the discharge orifice. Liquid is discharging, but the accumulation of air in the downstream surge volume is tending to drive the liquid level downward. This pressure is transmitted back through the process equipment, causing the liquid flow to decelerate—i.e., the level rises into the upstream surge space. Eventually, the downstream liquid level falls below the discharge orifice and the accumulated air is able to discharge. This results in a rapid decrease of the downstream surge pressure, which in turn causes the liquid in the process equipment to accelerate forward until the level is again above the orifice. The continuing oscillations caused in this way can be regarded as a relaxation process, the period depending mainly on the inertia of the liquid and the compressibility of the air in the upstream and downstream surge volumes. In certain cases, there was a tendency toward steady two-phase discharge rather than alternating discharge of air and water.

Measurement of Variables

The fixed and independently variable experimental quantities are summarized in Table I, with the estimated measurement accuracy.

The length of the liquid-filled connecting pipe between the surge volumes was taken for the case where the upstream and downstream liquid levels were level with the discharge orifice—i.e., $X_U = X_D = 0$. The same convention was used in defining the surge volumes. The overall friction factor, F, is expressed in terms of the pressure drop between the upstream and downstream surge tanks. It was measured at steady-flow conditions and within experimental limits was independent of flow rate. It takes into account the effects of bends, enlargements, etc., as well as pipe wall friction in the "process" pipe. The gate valve enables F to be varied.

Provision was made to have the discharge orifices

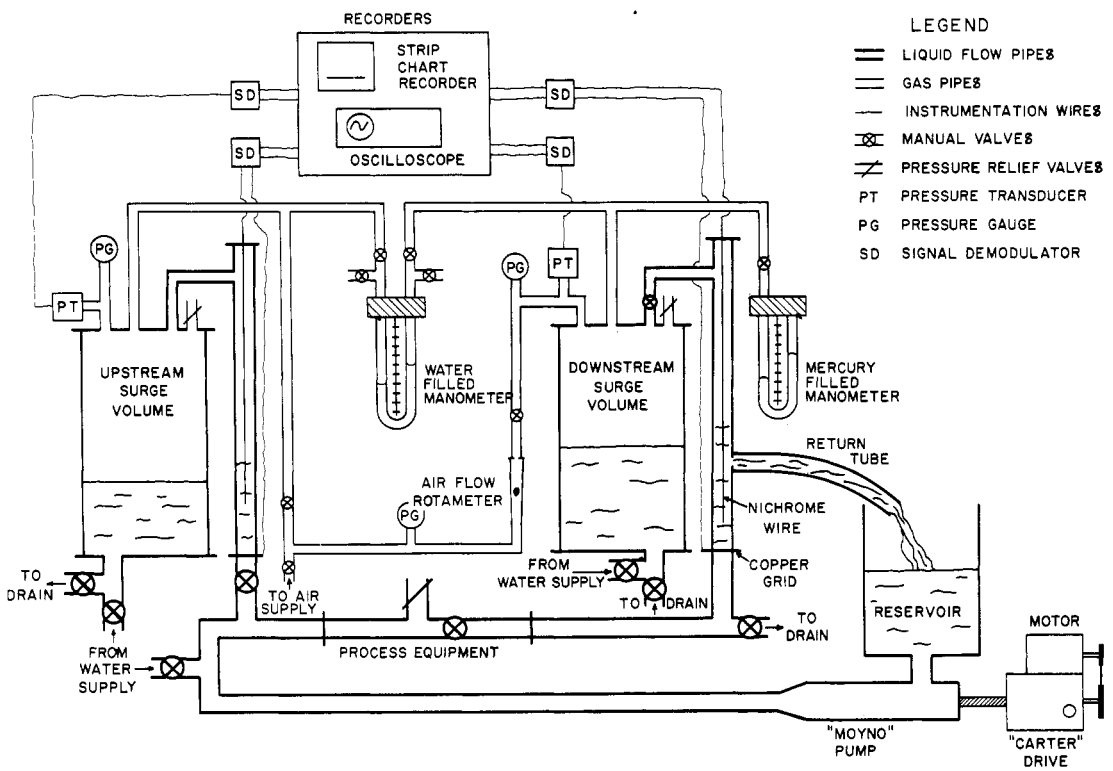

Figure 1. Experimental apparatus

interchangeable. Their effective discharge areas were determined by steady-flow experiments with water; the areas were calculated from the measured back-pressure developed, assuming no contraction. The same assumption is made in the later calculations (see Equation 4, etc.). The time-average water flow rate was determined from the speed of the rotary pump, while the air flow was metered on a rotameter at the line pressure of 110 psig. The air rate was controlled by a needle valve and because of the large pressure drop involved the rotameter reading was unaffected by the pressure fluctuations in the downstream surge tank. The period of the liquid pulsations was measured to within ±1% by timing 10 cycles with a stopwatch. The maximum and minimum liquid levels in upstream and downstream glass connecting pipes were measured to within ±⅛ inch by eye, with a scale fixed to the pipe wall.

The liquid level wave forms were measured electrically using two parallel Nichrome wires with a high resistance (690 ohms per foot) immersed in the water. A small amount of sodium chloride was added to the water, lowering its resistance to 150 ohms between the wires. In this way, the liquid level acted as a sliding short-circuit on the Nichrome wires. Polarization effects were reduced by applying a high frequency a.c. voltage across the Nichrome wires and subsequently rectifying the signal for showing on the oscilloscope screen. Unfortunately, the calibration of this technique against the cinecamera record was not conclusive.

More satisfactory wave-form measurements were obtained from the upstream and downstream surge tank pressures, using diaphragm-type transducers (Pace Engineering Co.). The output was recorded on a Honeywell Visicorder.

Theory

In the work of Baird (1967), an attempt was made to predict the performance of this type of pulsator analytically. It was possible to predict the operating frequency to within about ±15%, but the amplitude could not be worked out analytically from first principles, and an empirical correlation was necessary. The reasons for this limitation are that the system is nonlinear, with square-law frictional damping at the discharge orifice, and with a discontinuity in the downstream pressure wave form whenever the liquid level passes the discharge.

In this paper, the equations of the system are solved numerically by a Runge-Kutta routine. First, it is necessary to state the basic equations.

Mass Balances. The water is assumed incompressible over the pressure range encountered. Thus the mass balance at the tee-piece upstream of the process equipment may be written volumetrically:

$$Q_L = A_I U_I + A_U \frac{dX_U}{d\theta} \tag{1}$$

The liquid discharge rate, Q_{OL}, from the orifice may be written similarly:

$$Q_{OL} = A_D\left(U_D - \frac{dX_D}{d\theta}\right) \tag{2}$$

Here, velocity U_D refers to the region below the discharge. Q_{OL} becomes zero whenever the liquid level is below the discharge—i.e., $X_D < 0$.

A third mass balance equation can be written for air. Here the units of volume flow are standard cubic feet. The accumulation of air in the surge volume is

$$\frac{dN}{d\theta} = Q_G - Q_{OG} \tag{3}$$

In this case, Q_{OG} becomes zero whenever $X_D > 0$.

Discharge through Orifice. The effective area, A_O, of the orifice is assumed the same for air and water. This water discharge rate is given approximately by

$$Q_{OL} = A_O\left[2(P_{DO} - P_A)/\rho_L\right]^{1/2} \tag{4}$$

Small corrections in the program were made by Milburn (1969) to allow for the liquid level and velocity upstream of the orifice. The same form of equations could be written for air at very low pressure differences. In general, however, the equation for subsonic isentropic discharge of an ideal gas is used:

$$Q_{OG} = A_O\left\{2P_D\left(\frac{\gamma}{\gamma-1}\right)\left(\frac{P_A}{P_D}\right)^{1/\gamma} \times \left[1 - \left(\frac{P_A}{P_D}\right)^{(\gamma-1)/\gamma}\right]/\rho_{GA}\right\}^{1/2} \tag{5}$$

The upper limit on Q_{OG} is given by the equation for sonic flow.

$$Q_{OG} = \frac{A_{OG}\rho_{GA}}{\rho_{GD}}\left(\frac{2\gamma R T_D}{\rho_{GA}}\right)^{1/2}\left(\frac{2}{\gamma+1}\right)^{1/(\gamma-1)} \tag{5a}$$

Balance of Pressures. The pressure difference between the upstream and downstream surge tanks is balanced by frictional and inertial pressures, and by a small gravitational term due to imbalance between the liquid levels.

$$P_U - P_D = F|U_T|U_T + \rho_L\Sigma\left[L(dU/d\theta)\right] + \rho_L(X_D - X_U)g \tag{6}$$

Table I. Major Experimental Quantities

Upstream surge volume, V_U, ft³	0.2, 0.4, 0.8		±0.004
Downstream surge volume, V_D, ft³	0.2, 0.4, 0.8		±0.004
"Process" pipe, nominal diam., inches	¾	2	
"Process" pipe, cross-section area[a], ft²	0.00371	0.0233	
"Process" pipe, length, ft	3.72	3.33	
Connecting pipes			
Cross-section area (glass), ft²	0.0220		
Length (glass)[b], ft	7.5		
Cross-section area (steel)[a], ft²	0.0233		
Length (steel), ft	5.98		
Over-all friction factor	0.0001 to 0.005 inch water per (lb/min)² ±10%		
Discharge orifices			
Nominal diameter, inch	¼	½	¾
Equivalent Area, A_O, in.²	0.042	0.146	0.355
Water flow rate ranges, Q_l lb/min ± 1%	20–40	20–120	74–360
Air flow rate ranges, Q_G, std ft³/sec ±2%	0.011–0.071	0.011–0.118	0.011–0.153

[a] Values from standard tables for Schedule 40 pipe. [b] Length occupied by water in no-flow situation ($X_U = 0 = X_D$). Pipework above this level considered part of surge volume.

The dimensional friction factor, F, is defined in terms of U_T. The modulus enables the frictional term to change sign according to the flow direction. The inertial term is the sum of the inertias in the various pipe sections, with the accelerations found by continuity from the acceleration $dU_T/d\theta$ in the main pipe section.

Equation of State of Gas in Surge Tanks. The changes in liquid level X_U and X_D are accompanied by corresponding pressure changes. Consider first the upstream surge volume:

$$P_U(V_U - A_U X_U)^k = \text{constant} \tag{7}$$

The value of exponent k is not necessarily equal to γ.

In the downstream surge tank, the quantity of air, N (as standard cubic feet), occupies a volume $(V_D - A_D X_D)$. The equation of state may be written

$$P_D\left(\frac{V_D - A_D X_D}{N}\right)^k = \text{constant} \tag{8}$$

This equation is valid, even though N is a function of time, as the bracketed term is proportional to the specific volume of the gas.

Solution of Equations. The foregoing equations include four first-order differential equations in time. Equations 1 and 2 can be solved for the rate of change of upstream and downstream liquid level, while Equation 3 refers to the change in the amount of gas in the downstream surge. Equation 6 can be solved for the liquid accelerations $dU/d\theta$ in the process equipment and connecting lines.

These equations were solved numerically by a third-order Runge-Kutta technique. Only a rough estimate of initial conditions was necessary, and the calculation was continued until the oscillations in pressures, liquid levels, etc., repeated themselves regularly. The parameters for convergence were the repeatability of the upstream level extrema and the period. In some cases, convergence was not obtained in the specified length of simulated time; convergence was assumed, however, and an error message was printed out. Once a converged solution was obtained or assumed, the calculated values of pressures, volumes, and flows were stored for an integration routine. A second indication of convergence was obtained by comparing the integrated average outflows with the known inflows of gas and liquid. The program also calculated the ratio of the time-average absolute Reynolds number to the steady-flow Reynolds number in the "process equipment." This ratio is a measure of the additional turbulence created by pulsation and available to increase the rate of a transport process.

Results

Equation of State of Gas in Surge Volumes. Exponent k in Equations 7 and 8 is not necessarily the ratio γ of specific heats of the gas. In principle, k could have any value between unity for isothermal conditions and 1.4 for adiabatic conditions. The data from 165 experiments were analyzed to obtain a realistic value of k for the upstream volume. The upstream pressure and liquid level fluctuations were measured during oscillatory operation of the system, and Equation 7 was solved for k.

$$k = \frac{\ln[P_{U\text{Max}}/P_{U\text{Min}}]}{\ln[V_{U\text{Max}}/V_{U\text{Min}}]} \tag{7a}$$

The average value of k was 1.43, with a standard deviation of ± 0.20. This led to the assumption in the numerical simulation that $k = 1.4$—i.e., the air behaved adiabatically. However, in a few cases transient mist formation was observed in the surge tanks. This, and the fact that the deviation was much larger than that expected from measurement error, suggest a more complex behavior in reality.

Irregular Pulsations. The majority of the 165 experiments carried out (range of conditions as in Table I) gave "regular" pulsations—i.e., the single maxima and minima in liquid level and surge tank pressure repeated themselves in successive cycles. However, in some cases the pulsations repeated themselves with more than one maximum and minimum—"multiple pulsations." In some other cases, the pulsations were completely nonreproducing. These irregular pulsations occurred when the discharge from the orifice was of a two-phase nature for a large part of the time.

Repeatability of Experiments. Twenty-seven experiments giving regular pulsations were repeated later under the same conditions. One experiment was in considerable disagreement and was discarded. Of the remainder, 8% of the maximum-minimum pressure measurements and 9% of the liquid level amplitude measurements did not reproduce within the estimated experimental error. Only one of the measured periods differed by more than 0.03 second and three by more than 0.02 second.

Two-Phase Discharge. It was observed experimentally that appreciable two-phase discharge occurred, contrary to the assumptions made following Equations 2 and 3.

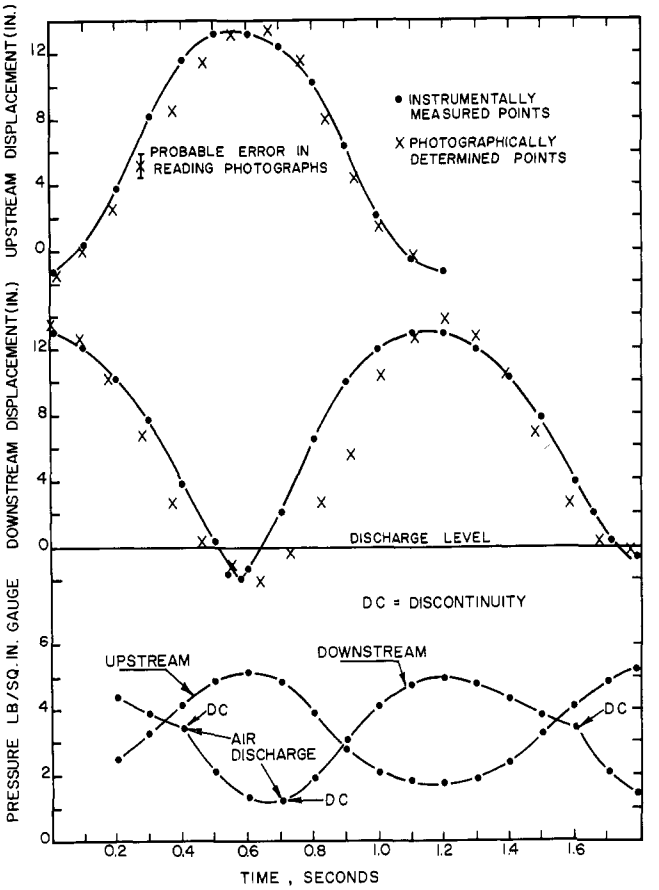

Figure 2. Typical measured variations of liquid level and pressure with time

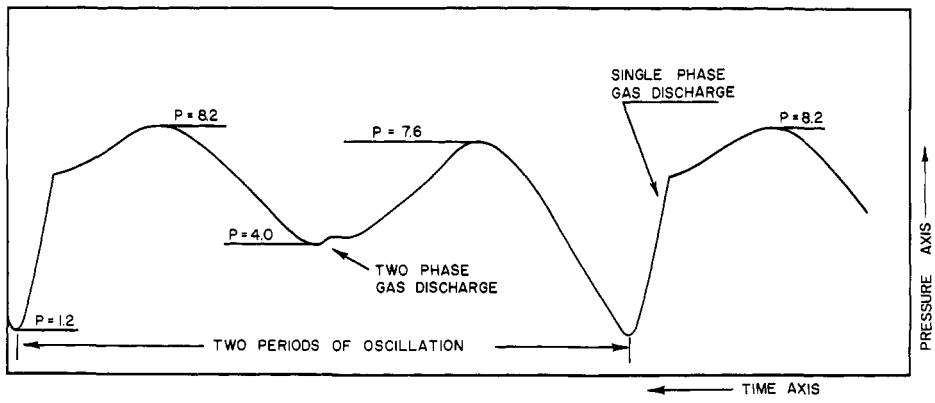

Figure 3. Example of measured multiple pulsation wave form: downstream pressure vs time
Pressures given in pounds per square inch gage

Moreover, preliminary calculations of liquid level amplitude tended to be greater than the observed values.

A simple method of allowing for this is to consider the intersection of the circular discharge orifice by the planar liquid level. In this way, the fraction of the discharge area available for gas discharge would be

$$A_{OG}/A_O = \tfrac{1}{2} - 2/\pi \sin^{-1}(y) - y(1 - y^2)^{1/2}/\pi \quad (9)$$

The limits of this expression are, of course, $-1 \leq y \leq 1$. Unfortunately, Equation 9 is not adequate, as it was observed that two-phase discharge occurred in some cases when the liquid level was above the top of the discharge. Detailed observation of this phenomenon was difficult, but it was thought that the liquid surface near the discharge was distorted by the flow of air toward the discharge, in the same way as it occurs just below the flooding point in a packed tower. An approximate expression for the area for gas discharge was postulated by Milburn (1969) in terms of gas and liquid Froude numbers. This permitted some gas discharge for values of X_D less than 0.07 foot, a figure selected as a reasonable upper limit for the surface distortion effect. The area calculated in this way was added to the area given by Equation 9.

Wave Forms. The performance of the pulsator for a typical case is illustrated in Figure 2, which shows X_U, X_D, P_U, and P_D as functions of time. Displacements X_U and X_D were measured photographically as well as by the conductivity method; agreement between the methods is not very good. The direct photographic method is believed to give the more accurate curve.

As may be expected, the upstream and downstream liquid displacement curves are about 180° out of phase. The upstream pressure curve is nearly sinusoidal and similar in form to the upstream displacement curve, in accordance with Equation 7 relating X_U and P_U. The downstream pressure curve shows a discontinuity at 0.41 second, corresponding to the start of gas discharge. This change occurs about 0.06 second before the downstream level reaches the orifice center line, illustrating the premature discharge referred to above.

In Figure 3, a typical wave form for "multiple pulsation" is illustrated, showing two maxima and two minima. The shallower of the two minima was accompanied by two-phase discharge, while the lower minimum corresponded to discharge of gas alone.

Typical Data Compared with Calculation. Figure 4 shows the effect of gas rate on the liquid displacement extrema, pressure extrema, and period. The amplitude, defined here as the difference between the displacement extrema, increases rapidly at first and then more slowly. A similar effect was seen in the earlier work by Baird (1967) at lower amplitudes. In this case the numerical calculation somewhat underestimates the amplitudes. The upstream and downstream pressure extrema agree fairly well with calculation, as does the period of pulsation. The period is only slightly affected by the gas rate.

The effect of varying liquid rate at constant gas rate is illustrated in Figure 5. At very low liquid rates, considerable two-phase discharge was seen. The observed and calculated periods do not agree very well in this case. As the liquid flow increases, a maximum displacement amplitude (both observed and calculated) occurs. At the highest liquid flows, there is again a tendency toward two-phase discharge and the amplitudes decrease. On the whole, the numerical technique predicts these performances reasonably well, with a tendency to underestimate amplitude.

It is interesting to compare the time-average absolute Reynolds numbers in pulsed flow with the Reynolds number corresponding to steady flow. For the three experimental points given in Figure 4 the Reynolds number for the steady component of flow is 12,264. However,

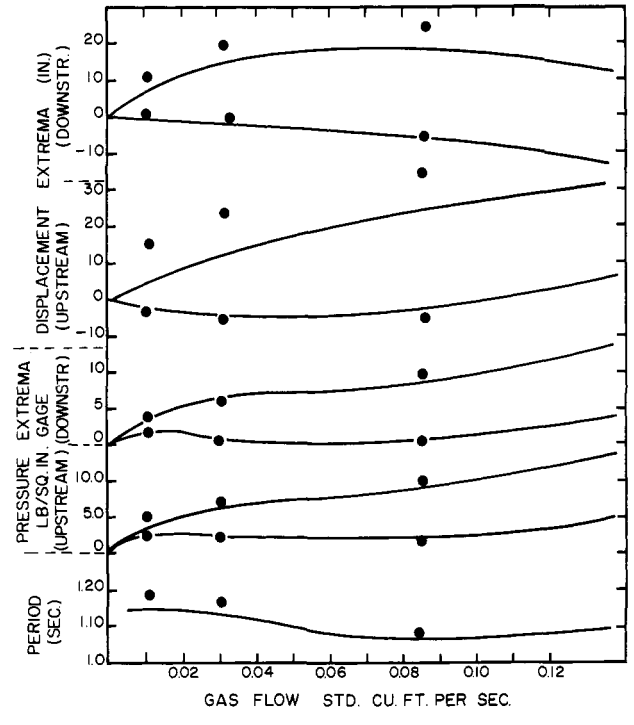

Figure 4. Effect of air flow on pulsation characteristics
Surge volumes 0.2 ft.^{3} Liquid flow 80 pounds per minute. Orifice nominal diameter 1/2 inch. Test section 2-inch pipe
● Experimental points
— Theoretical prediction

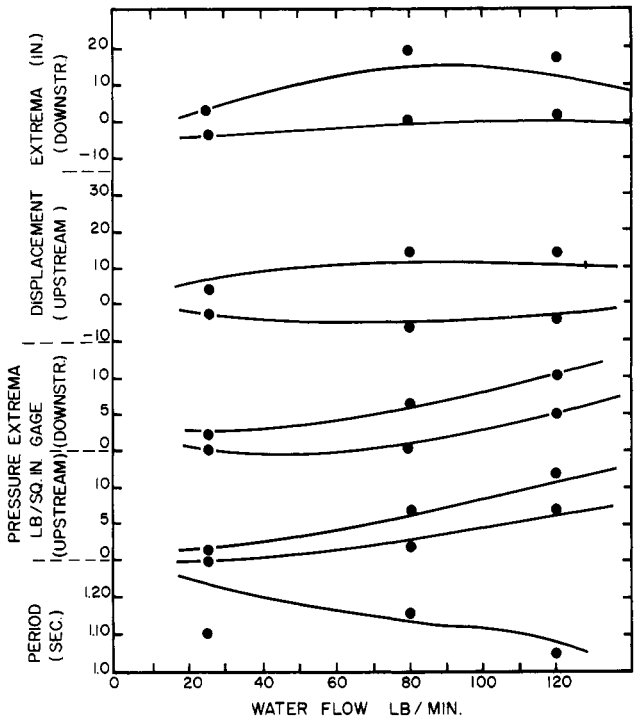

Figure 5. Effect of water flow on pulsation characteristics
Air flow 0.0308 std. ft.^{3} per second. Other conditions and symbols as in Figure 4

the calculated time-averaged absolute values are 16,714, 34,002, and 53,807 in order of increasing gas flow rate. These much higher values are, of course, due to flow reversal—for example, at the highest gas rate of 0.085 std. ft.^{3} per second, the Reynolds number ranged between 82,913 in the forward direction and 53,527 in the reverse direction. Such a pronounced flow reversal is likely to increase heat transfer rates considerably, as suggested by Lemlich (1961).

All Data Compared with Calculation. For each measured and calculated quantity a percentage deviation can be defined as follows:

$$100\left[\frac{\text{calcd. value} - \text{exptl. value}}{\text{exptl. value}}\right]$$

Figure 6 shows bar charts of percentage deviation for downstream amplitude and period, for all 165 experiments done. The present method seriously underestimates the amplitude in over 60 cases—i.e., too much two-phase flow is assumed to occur. In fact, in 29 cases the numerical simulation degenerated after a time into steady two-phase discharge—i.e., zero amplitude. It might have been possible to adjust the coefficients of the two-phase discharge equation, so as to obtain a better fit with the data, but in any case the model was an approximate one. In its present form, the program has the practical virtue of giving conservative values.

The calculated periods were also, on average, smaller than the observed values, although the difference was less pronounced than in the case of displacement amplitude.

Stability of Pulsations. The problem of two-phase discharge is particularly important in deciding whether pulsation will occur, and if so whether the pulsations will be regular or irregular. At either very high or very low liquid

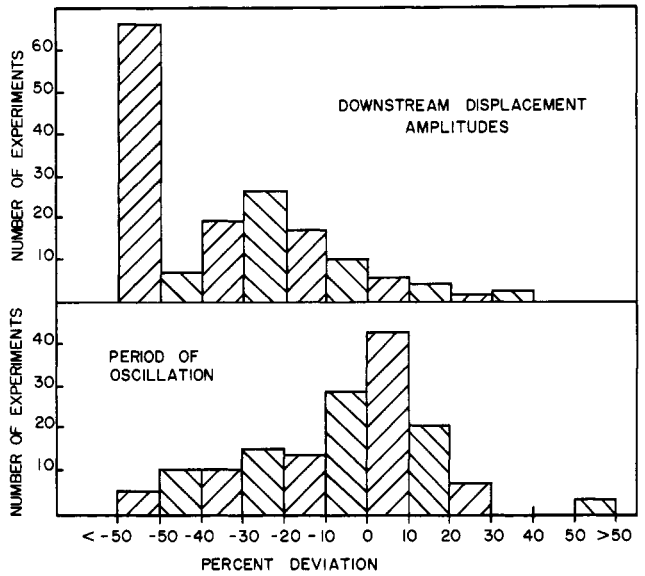

Figure 6. Distribution of deviations for downstream displacement amplitude and period of oscillation

to gas flow ratios, two-phase discharge will occur, with the less important phase being bled through the orifice in a stream of the major phase. At intermediate flow ratios, pulsation is most likely to occur, and indeed a maximum amplitude is observed in Figure 5. The effect of increasing orifice size is to encourage two-phase discharge—i.e., to reduce the tendency toward spontaneous pulsation. For example, it was difficult within the range of flow rates available to obtain regular pulsations with the ¾-inch discharge. In most cases with the ½-inch discharge and in all cases with the ¼-inch discharge, regular pulsations were obtained. However, as the discharge size is reduced, the over-all pressure drop increases. A practical solution might be to have discharge through multiple small orifices or a horizontal slit milled into the rise tube. Another possibility is to reduce the diameter of the downstream riser tube, so that the liquid level moves more rapidly past the orifice and the two-phase discharge is reduced. These ideas cannot, however, be quantified in the absence of a better understanding of two-phase discharge.

Conclusions

The advantages of the pulsation technique are the relatively low capital cost of the equipment, and the reliability of its operation, provided the discharge orifice is correctly sized. The supply pressures of the air and water must, of course, be greater than the maximum pressure reached in the pulsation cycle, so the major cost item will be the power required for compression of the air and for boosting the water pressure if necessary. These costs must be set against the economic gains of pulsed operation (due to higher heat or mass transfer, etc.) in any particular case.

Nomenclature

A = cross-sectional area, ft^2
D = diameter, ft
F = friction factor, Equation 6
g = gravitational acceleration, ft sec^{-2}
k = exponent in Equation 7

L = length of pipeline, ft
N = volume of gas (at standard conditions) in downstream surge, ft^3
P = pressure, $lb_m\ ft^{-1}\ sec^{-2}$
Q = volume flow rate (at standard conditions), $ft^3\ sec^{-1}$
R = gas constant, $lb_m\ ft^{-1}\ sec^{-2}\ °K^{-1}$
T = absolute temperature, °K
U = liquid phase velocity, $ft\ sec^{-1}$
V = volume of surge space, ft^3
X = liquid level, ft
y = $2X_D/D_O$

GREEK LETTERS

γ = ratio of specific heats (= 1.4 for air)
ρ = density, $lb_m\ ft^{-3}$
θ = time, seconds

SUBSCRIPTS

A = atmospheric conditions
D = downstream
L = liquid phase
G = gas phase
O = orifice
T = test section
U = upstream
I = connecting pipes

Literature Cited

Baird, M. H. I., *Brit. Chem. Eng.* **11**, 20 (1966).
Baird, M. H. I., *Brit. Chem. Eng.* **12**, 1877 (1967).
Baird, M. H. I., Gloyne, A. R., Meghani, M. A. N., *Can. J. Chem. Eng.* **46**, 249 (1968).
Lemlich, R., *Chem. Eng.* **68**, (10), 171 (1961).
McGurl, G. U., Maddox, R. N., IND. ENG. CHEM. PROCESS DES. DEVELOP. **6**, 6 (1967).
Martinelli, R. C., Boelter, L. M. K., Weinberg, E. B., Yakahi, S., *Trans. A.S.M.E.* **65**, 789 (1943).
Massimilla, L., Volpicelli, G., Raso, G., *Chem. Eng. Progr. Symp. Ser.* **62** (62), 63 (1966).
Milburn, C. R., M. Eng. thesis, McMaster University, Hamilton, Canada, 1969.
Thornton, J. D., *Chem. Eng. Progr. Symp. Ser.* **13**, 39 (1954).
Van Dijck, W. J. D., U.S. Patent **2,011,186** (August 1935).
Ziolkowski, Z., Filip, S., *Int. Chem. Eng.* **3**, 433 (1963).

RECEIVED for review January 12, 1970
ACCEPTED May 15, 1970

62nd Annual Meeting, A.I.Ch.E., Washington, D. C., November 16-20, 1969. The authors are grateful to the National Research Council of Canada for financial support of this work.

Carbon Distribution Functions in a Fluid Catalytic Cracker

S. M. Jacob

Research Department, Mobil Research & Development Corp., Paulsboro, N. J. 08066

An iterative computational method was developed to obtain the carbon distribution functions for a fluid catalytic cracker. The FCC unit was idealized as a three-vessel system consisting of a backmixed regenerator, a plug flow riser reactor, and a backmixed reactor.

In a TCC unit the catalyst is burned essentially clean of carbon on leaving the regenerator. In contrast, because of extensive catalyst mixing, particles leaving an FCC regenerator vary in carbon content. Thus, samples of circulating FCC catalyst show wide carbon distributions, while those from a TCC unit have more uniform carbon content. The practical significance of such carbon distributions is that the yield, selectivity, and aging characteristics of a catalyst particle are affected by the amount of carbon present. Furthermore, the heat balance in an FCC unit is more sensitive to coke on catalyst than in a TCC unit which has catalyst cooling coils as a heat sink.

An analytical solution was available in the literature for carbon distribution in a system of two perfectly stirred vessels, one acting as a carbon former and the other as a carbon remover. The current work extends this analysis to the case where a riser or plug flow reactor section is also present. The addition of a riser is important, since carbon distributions are profoundly affected by the presence of this plug flow section.

This paper provides a tool for describing the carbon distribution in fluid catalytic cracking units. The regenerator is considered to be a perfectly mixed vessel in which the carbon on the catalyst is burnt off. Carbon is deposited in a plug flow riser reactor and a backmixed reactor, in that order.

Carbon on each catalyst particle grows or is removed according to some prescribed differential law. In the reactor, the rate of carbon deposited is represented by the coking law for a specific crude. In the regenerator, carbon removal is measured by the rate at which it is burnt off.

Discussion

Mathematical Development. For a perfectly mixed vessel continuously fed and depleted by a stream of particles,